

Configurational entropy of tachyon kinks on unstable Dp-branes

Chong Oh Lee*

Department of Physics, Kunsan National University, Kunsan 573-701, Republic of Korea

We consider tachyon effective theory with Born-Infeld electromagnetic fields and investigate the configurational entropy of the various tachyon kink solutions. We find that the configurational entropy starts at a minimum value and saturates to a maximum value as the negative pressure of pure tachyonic field increases. In particular, when an electric field is turned on and its magnitude is larger than or equal to the critical value, we find the configurational entropy has a global minimum, which is related to the predominant tachyonic states.

I. INTRODUCTION

The investigation of a D-brane with tachyon condensation [1] has opened up a new window to explore off-shell structure of string theory. It was found that rolling tachyon solutions through boundary conformal field theory and effective field theory describe the motion of the tachyon on unstable D-branes [2–4]. It was extensively studied for the inhomogeneous tachyon condensation [5–8], the emission of closed string radiation [9, 10] and for instability of codimension-one D-branes [9, 11–13].

It was found that the configurational entropy represents the informational content in physical systems with localized energy density configurations through measure of their ordering in field configuration space [14, 15]. It was extensively studied for AdS/QCD holographic models [16–22] and for instability of a variety of physical systems [15–17, 23–29]. In particular, the configurational entropy was investigated for dynamical tachyonic AdS/QCD holographic model. The authors showed that the corrections to dual mesonic states in the boundary QCD due to tachyonic fields become more dominant their states [19]. Since decay of unstable D-branes has rich tachyon kink solutions, it is intriguing to calculate the configurational entropy of tachyon kink solutions.

The paper is organized as follows: in the next section we will investigate configurational entropy in tachyon effective theory with Born-Infeld electromagnetic fields. Firstly, we will calculate the configurational entropy in the pure tachyon case. Next, we will turn on electric/electromagnetic field. Then the configurational entropy will be computed. We will also discuss their configurational entropy by varying the electromagnetic field. In the last section we will give our conclusion.

II. CONFIGURATIONAL ENTROPY OF TACHYON KINKS

The Boltzmann-Gibbs entropy S_{BG} is defined as

$$S_{BG} = -k_B \sum p_i \ln p_i, \quad (2.1)$$

with $\sum p_i = 1$. In fact, it is given as the most general formula between the entropy and the set of probabilities of their microscopic states in statistical thermodynamics. Here, k_B is the Boltzmann constant, and p_i the probability of a microstate, respectively. In particular, when each microstate has equal probability as the following

$$p_i = \frac{1}{W}, \quad (2.2)$$

with the number of microstates W , S_{BG} (2.1) reduces to the configurational entropy S_C in the microcanonical ensemble

$$S_C = k_B \ln W, \quad (2.3)$$

since W can be treated as the number of possible configurations at a given energy. For example, there are two different molecules with the total number of molecules N_0 , then the number of one type of molecule is N_1 and the number of another type of molecule N_2 . One obtains the configurational entropy S_C

$$S_C = k_B \ln W = k_B \ln \left(\frac{N_0!}{N_1! N_2!} \right), \quad (2.4)$$

and after employing Sterling's approximation $\ln N! \approx N \ln N$, one has

$$S_C = k_B (N_0 \ln N_0 - N_1 \ln N_1 - N_2 \ln N_2). \quad (2.5)$$

As another example, there is the system with spatially localized energy in d -dimensional space. When its energy density is given as a function of the position $\rho = \rho(x)$, the energy density is written as

$$\rho(k) = \left(\frac{1}{\sqrt{2\pi}} \right)^d \int \rho(x) e^{-ik \cdot x} d^d x \quad (2.6)$$

through the Fourier transform and the modal fraction reads

$$f(k) = \frac{|F(k)|^2}{\int |F(k)|^2 d^d k}, \quad (2.7)$$

which measures the relative weight of a given mode k . One defines the configurational entropy $S_C[f]$ as

$$S_C[f] = - \sum_{l=1}^n f_l \ln(f_l). \quad (2.8)$$

* cohlee@gmail.com

and in the limit of $n \rightarrow \infty$, one has [23, 24]

$$S_C[f] = - \int_{-\infty}^{\infty} g(k) \ln[g(k)] d^d k, \quad (2.9)$$

where $g(k) = f(k)/f(k)_{\max}$ and the maximum modal fraction $f(k)_{\max}$.

One introduces a runaway tachyon potential¹

$$V(T) = \frac{1}{\cosh(T/T_0)}, \quad (2.10)$$

with $T_0 = \sqrt{2}$ for the non-BPS D-brane in the superstring and $T_0 = 2$ for the bosonic string. The effective tachyon action for the unstable D3-brane system with the tension of the D3-brane \mathcal{T}_3 is given by [1–4]

$$S = -\mathcal{T}_3 \int d^4 x V(T) \sqrt{-X}, \quad (2.11)$$

with

$$X = \det(\eta_{\mu\nu} + \partial_\mu T \partial_\nu T + F_{\mu\nu}) \quad (2.12)$$

which leads to equations of motion for the gauge field A_μ and for the tachyon T

$$\partial_\mu \left(\frac{V(T)}{\sqrt{-X}} C_A^{\mu\nu} \right) = 0, \quad (2.13)$$

$$\partial_\mu \left(\frac{V(T)}{\sqrt{-X}} C_S^{\mu\nu} \partial_\nu T \right) + \sqrt{-X} \frac{dV(T)}{dT} = 0. \quad (2.14)$$

Here $C_A^{\mu\nu}$, and $C_S^{\mu\nu}$ are asymmetric and symmetric part of the cofactor,

$$C_A^{\mu\nu} = \bar{\eta}(\bar{F}^{\mu\nu} + \bar{\eta}^{\mu\alpha} \bar{\eta}^{\beta\gamma} \bar{F}_{\alpha\beta}^* \bar{F}_{\gamma\delta}^* \bar{F}^{\delta\nu}), \quad (2.15)$$

$$C_S^{\mu\nu} = \bar{\eta}(\bar{\eta}^{\mu\nu} + \bar{\eta}^{\mu\alpha} \bar{\eta}^{\beta\gamma} \bar{\eta}^{\delta\nu} \bar{F}_{\alpha\beta}^* \bar{F}_{\gamma\delta}^*) \quad (2.16)$$

with determinant of barred metric $\bar{\eta}$

$$\bar{\eta} = -(1 + \partial_\mu T \partial^\mu T), \quad (2.17)$$

and inverse metric $\bar{\eta}^{\mu\nu}$

$$\bar{\eta}^{\mu\nu} = \eta^{\mu\nu} - \frac{\partial^\mu T \partial^\nu T}{1 + \partial_\alpha T \partial^\alpha T}. \quad (2.18)$$

Here, contravariant barred field strength tensor $\bar{F}^{\mu\nu}$ denotes

$$\bar{F}^{\mu\nu} = \bar{\eta}^{\mu\alpha} \bar{\eta}^{\nu\beta} \bar{F}_{\alpha\beta}, \quad (2.19)$$

and barred field strength tensor $\bar{F}_{\mu\nu}$

$$\bar{F}_{\mu\nu} = F_{\mu\nu}, \quad (2.20)$$

and its dual field strength $\bar{F}_{\mu\nu}^*$

$$\bar{F}_{\mu\nu}^* = \frac{1}{2} \bar{\epsilon}_{\mu\nu\alpha\beta} \bar{\eta}^{\alpha\gamma} \bar{\eta}^{\beta\delta} \bar{F}_{\gamma\delta}. \quad (2.21)$$

Energy-momentum tensor $T_{\mu\nu}$ is obtained as [11, 12]

$$T^{\mu\nu} = \mathcal{T}_3 \frac{V(T)}{\sqrt{-X}} C_S^{\mu\nu}. \quad (2.22)$$

One considers the tachyon field $T(x)$ as the function of the spatial coordinate x , electric field $\mathbf{E}(x)$ and the magnetic field $\mathbf{B}(x)$. Then through solving Eq. (2.13), one obtains that

$$\tau \equiv \mathcal{T}_3 \frac{V(T)}{\sqrt{-X}}, \quad (2.23)$$

with $\tau = \text{constant}$, which leads to a single first-order equation

$$\mathcal{E} = \frac{1}{2} T'^2 + U(T), \quad (2.24)$$

with

$$\mathcal{E} = -\kappa/(2\lambda) \quad (2.25)$$

and

$$U(T) = -(\mathcal{T}_3 V(T))^2 / (2\lambda\tau^2). \quad (2.26)$$

Here κ and λ are

$$\kappa = 1 - \mathbf{E}^2 + \mathbf{B}^2 - (\mathbf{E} \cdot \mathbf{B})^2, \quad (2.27)$$

$$\lambda = 1 + B_1^2 - E_2^2. \quad (2.28)$$

A. Tachyon kink case

When the tachyon field and the abelian gauge field are given as the function of the position $T(x)$ and $F_{\mu\nu}(x)$, profiles of tachyon field $T(x)$ on general unstable Dp-brane are the same to that on unstable D2-brane [12]. For simplicity, we consider from now on tachyon effective theory with Born-Infeld electromagnetic fields in three-dimensional spacetime and investigate the configurational entropy of the various tachyon kink solutions.

In the case of pure tachyon model, the Born-Infeld type effective action (2.11) reduces to the following action²:

$$S = -\mathcal{T}_2 \int d^3 x V(T) \sqrt{-\det(\eta_{\mu\nu} + \partial_\mu T \partial_\nu T)}, \quad (2.29)$$

¹ For dS tachyon thick braneworld model, a more general tachyon potential $V(T)$ is given as [30]

$$V(T) = -\Lambda_5 \operatorname{sech}(\sqrt{-2\kappa_5^2 \Lambda_5/3} T) \sqrt{6 \operatorname{sech}^2(\sqrt{-2\kappa_5^2 \Lambda_5/3} T) - 1}$$

where Λ_5 is the five-dimensional bulk cosmological constant and κ_5 is the five-dimensional gravitational coupling constant.

² One considers generalization of the action to include the bulk action with the five-dimensional bulk cosmological constant

$$S = \int d^5 x \sqrt{-\det(g_{\mu\nu})} (R/2\kappa_5^2 - \Lambda_5) - \int d^5 x V(t) \sqrt{-\det(g_{\mu\nu} + \partial_\mu T \partial_\nu T)},$$

which leads to the energy density ρ [11, 12]

$$\rho \equiv T_{00} = \frac{-\mathcal{T}_2^2/p_1}{1 + \left[\left(\frac{\mathcal{T}_2}{p_1}\right)^2 - 1\right] \sin^2(x/T_0)}, \quad (2.30)$$

and the negative pressure p_1

$$p_1 \equiv T_{11} = -\mathcal{T}_2 \frac{V(T)}{\sqrt{1+T'^2}} < 0. \quad (2.31)$$

The mechanical energy \mathcal{E} (2.25) is given as $\mathcal{E} = -1/2$ and the potential $U(T)$ (2.26) is $U(T) = -(\mathcal{T}_2 V(T))^2/2$. Then, solutions are classified by $-p_1/\mathcal{T}_2$ and there are four possible cases: (i) When $-p_1/\mathcal{T}_2 > 1$, there is no motion. (ii) When $-p_1/\mathcal{T}_2 = 1$, there is hypothetical motion but the motion eternally stops at $U(0)$. (iii) When $-p_1/\mathcal{T}_2 < 1$, there is oscillatory motion. (iv) When $-p_1/\mathcal{T}_2 \rightarrow 0^+$, there is oscillatory motion with infinity period. Thus, we now calculate the configurational entropy of pure tachyonic field under $0 < -p_1/\mathcal{T}_2 < 1$.

The potential $U(T)$ (2.26) is explicitly obtained as

$$U(T) = -\frac{\mathcal{T}_2^2}{2p_1^2} \operatorname{sech}^2\left(\frac{T}{T_0}\right). \quad (2.32)$$

After taking $\mathcal{T}_2 = 1$, shapes of potential $U(T)$ for various values of the pressure p_1 are depicted in Fig. 1. The smaller the pressure $-p_1$ becomes, the more convex function in potential $U(T)$. Then, profiles of tachyon field $T(x)$ for various the pressure $-p_1$ and profiles of energy density are depicted in Fig. 2 and Fig. 3.

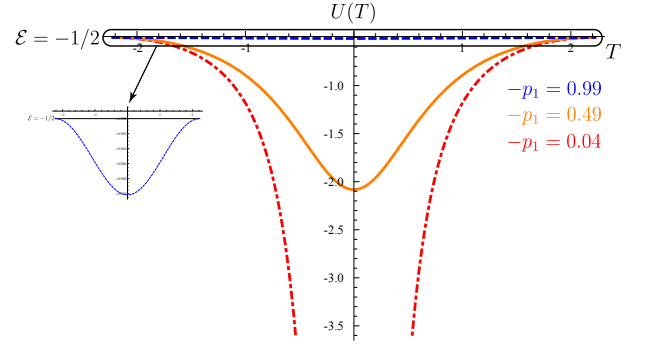


FIG. 1. Plot of potential $U(T)$ as the function of the tachyon field T (red dotted-dashed curve for the pressure $-p_1 = 0.04$, orange solid curve for the pressure $-p_1 = 0.49$, blue dashed curve for the pressure $-p_1 = 0.99$, respectively).

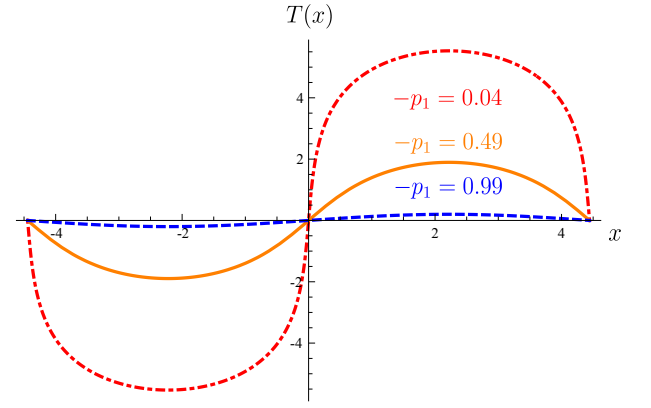


FIG. 2. Plot of the tachyon field $T(x)$ as the function of the position x (red dotted-dashed curve for the pressure $-p_1 = 0.04$, orange solid curve for the pressure $-p_1 = 0.49$, blue dashed curve for the pressure $-p_1 = 0.99$, respectively).

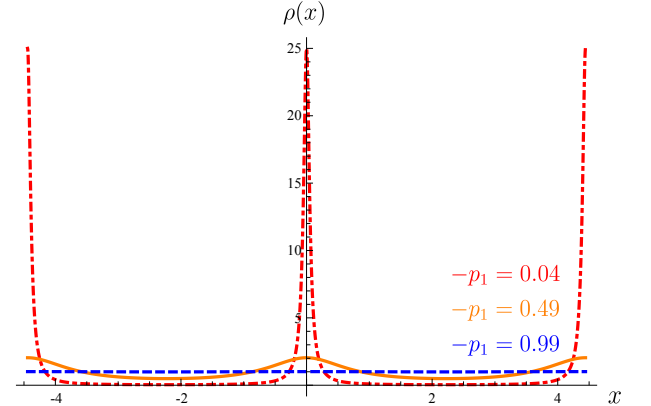


FIG. 3. Plot of energy density $\rho(x)$ as the function of the position x (red dotted-dashed curve for the pressure $-p_1 = 0.04$, orange solid curve for the pressure $-p_1 = 0.49$, blue dashed curve for the pressure $-p_1 = 0.99$, respectively).

which is adapted to a warped five-dimensional line element with an induced three-dimensional brane in a spatially flat cosmological background

$$ds^2 = e^{2f(\xi)}[-dt^2 + e^{2Ht}(dx^2 + dy^2 + dz^2) + d\xi^2],$$

with the warp factor $f(\xi)$ and the scale factor of the brane e^{Ht} , where H is integration constant, and one can get the following field equation [30]:

$$f'^2 + \frac{\kappa_5^2 \Lambda_5}{6} e^{2f} - H^2 = -\kappa_5^2 \frac{e^{2f} V(T)}{6\sqrt{1+e^{-2f} T'^2}}.$$

The five-dimensional gravitational coupling constant κ_5 is set to $\sqrt{6}$ and the above field equation in the absence of the negative bulk cosmological constant Λ_5 and the warp factor $f(\xi)$ reduces to the negative pressure (2.31) $p_1 = -\frac{V(T)}{\sqrt{1+T'^2}}$ with taking the tension of the D2-brane $\mathcal{T}_2 = 1$. Then the more general potential discussed in footnote 1, reduces exactly to the runaway tachyon potential (2.10) $V(T) = \frac{1}{\cosh(T/T_0)}$.

The configurational entropy of tachyon field $S_{C,T}$ is numerically calculated by Eqs. (2.6), (2.7), and (2.9), and is depicted in Fig. 4. As the negative pressure $-p_1$

grows up, $S_{C,T}$ starts at the minimum value ($S_{C,T} = 0.5441$) and saturates to the maximum value ($S_{C,T} = 1.7373$).

The momentum space plane waves with equally distributed modal fractions are sharply localized in position space while the momentum space singular modes broadly spreads out. Position space localized distributions have the maximum configurational entropy due to large amount of momentum modes while position space widespread distributions have the minimum configurational entropy due to small amount of momentum modes. Furthermore, the larger configurational entropy of physical system becomes, the larger its amount of energy to be generated. Thus in position space, the energy density with more sharply localized shape needs a larger amount of energy to be generated. On the contrary, the more energy density $\rho(x)$ in the presence of pure tachyonic fields sharply localized, the smaller the pressure $-p_1$ becomes while the more energy density $\rho(x)$ broadly spreads out, the bigger the pressure $-p_1$ becomes as shown in Fig. 3. As shown in Fig. 4, however, the above behaviour of configurational entropy by increasing the pressure $-p_1$ seems to be natural physically since the tachyon energy density with more widespread shape needs a larger amount of energy to be generated. In other words, this result is consistent with the fact that the configurational entropy grows up as the energy increases.

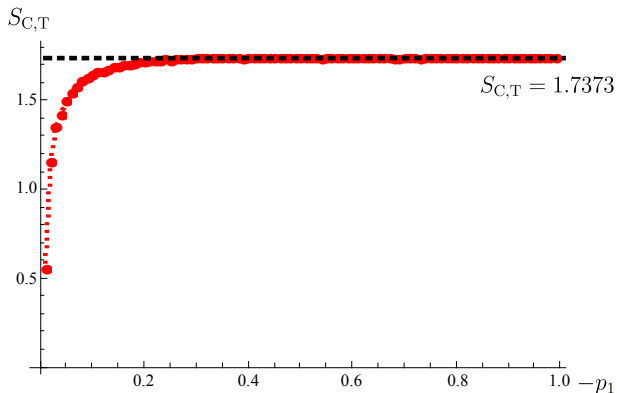


FIG. 4. Plot of tachyon configurational entropy $S_{C,T}$ as the function of the pressure $-p_1$.

B. Kink with electric field case

As discussed in the previous section we will apply a similar analysis to the kink with electric field case.

The energy density ρ is given as [11, 12]

$$\rho \equiv T_{00} = \Pi E + \frac{\mathcal{T}_2^2 E / \Pi}{1 + \left(\frac{\mathcal{T}_2^2 E^2}{\Pi^2 (1 - E^2)} - 1 \right) \sin^2(x\sqrt{1 - E^2}/T_0)}, \quad (2.33)$$

and conjugate momenta of the gauge field Π

$$\Pi = \mathcal{T}_2 \frac{V(T)}{\sqrt{-X}} E, \quad (2.34)$$

where E denotes the electric field. The mechanical energy (2.25) is given as

$$\mathcal{E}_E = -\frac{1}{2}(1 - E^2), \quad (2.35)$$

and the potential (2.26) is

$$U_E(T) = -\frac{\mathcal{T}_2 E^2}{2\Pi^2} V(T)^2 = -\frac{\mathcal{T}_2 E^2}{2\Pi^2} \frac{1}{\cosh^2(T/T_0)}. \quad (2.36)$$

Then, solutions are classified as \mathcal{E} or E . (i) When $\mathcal{E}_E < U_E(0)$ ($E^2 > 1/[1 + (\mathcal{T}_2/\Pi)^2]$), there is no motion. (ii) When $\mathcal{E}_E = U_E(0)$ ($E^2 = 1/[1 + (\mathcal{T}_2/\Pi)^2]$), there is hypothetical motion but the motion eternally stops at $U(0)$. (iii) $U_E(0) < \mathcal{E}_E < 0$ ($1/[1 + (\mathcal{T}_2/\Pi)^2] < E^2 < 1$), there is oscillatory motion. Thus, we will calculate the configurational entropy $S_{C,E}$ in the range $0 < E < 1$.

After employing $\mathcal{T}_2 = 1$, shapes of potential $U_E(T)$ for various values of electric field E are depicted in Fig. 5. The smaller electric field E becomes, the more convex function in potential $U_E(T)$. Then, profiles of tachyon field $T(x)$ for various electric field E and profiles of energy density are depicted in Fig. 6 and Fig. 7.

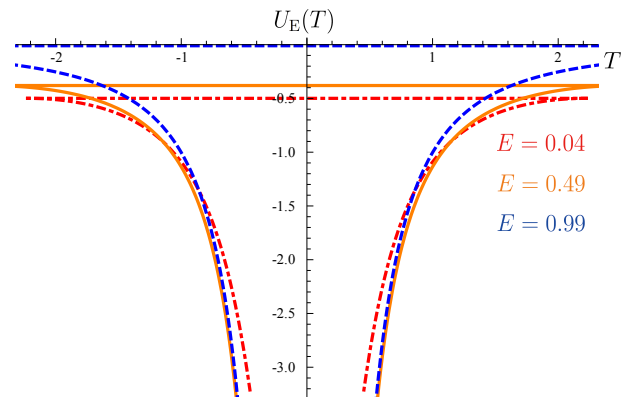


FIG. 5. Plot of potential $U_E(T)$ as the function of the tachyon field T (red dotted-dashed curve for electric field $E = 0.04$, orange solid curve for electric field $E = 0.49$, blue dashed curve for electric field $E = 0.99$, respectively).

After numerically evaluating Eqs. (2.6), (2.7), and (2.9), the configurational entropy $S_{C,E}$ is depicted in Fig. 8. Especially, as electric field E grows up, the configurational entropy reaches the minimum value ($S_{C,E} = 0.3485$) at a critical point ($E = 0.63$). In fact, the smaller configurational entropy of physical system becomes, the more dominant such physical system states since the larger its configurational entropy becomes, the larger its amount of energy to be generated. Thus, it is expected that the predominant tachyonic states happens at the minimum configurational entropy.

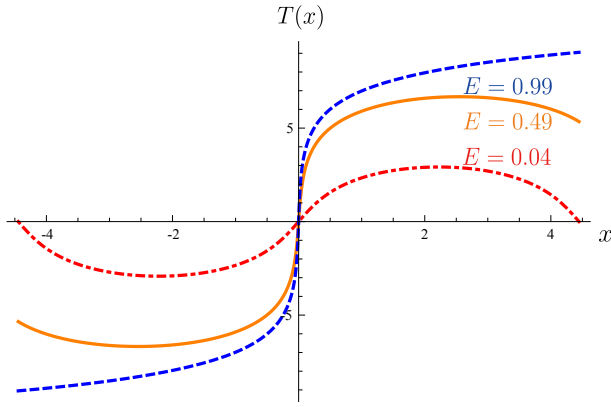


FIG. 6. Plot of the tachyon field $T(x)$ as the function of the position x (red dotted-dashed curve for electric field $E = 0.04$, orange solid curve for electric field $E = 0.49$, blue dashed curve for electric field $E = 0.99$, respectively).

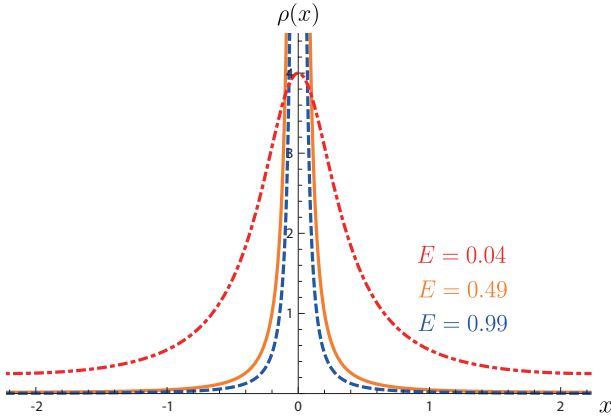


FIG. 7. Plot of energy density $\rho(x)$ as the function of the position x (red dotted-dashed curve for electric field $E = 0.04$, orange solid curve for electric field $E = 0.49$, blue dashed curve for electric field $E = 0.99$, respectively).

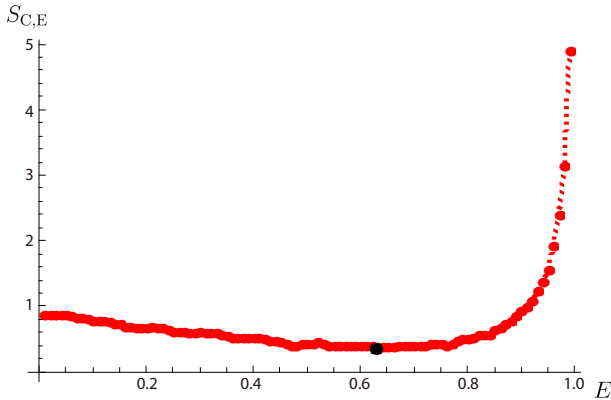


FIG. 8. Plot of tachyon configurational entropy with electric field $S_{C,E}$ as the function of electric field E .

C. Kink with electromagnetic field case

In the case of the kink with electromagnetic field, the energy density ρ is given as [11, 12]

$$\begin{aligned} \rho \equiv T_{00} &= \mathcal{T}_2 \frac{V(T)}{\sqrt{-X}} (1 + T'^2 + B^2) \\ &= \frac{\Pi_1(E_1^2 - B^2 E_2^2)}{E_1(1 - E_2^2)} + \frac{\mathcal{T}_2^2 E_1}{\Pi_1(1 - E_2^2)} V(T)^2. \end{aligned} \quad (2.37)$$

The mechanical energy (2.25) is given as

$$\mathcal{E}_{\text{EM}} = -\frac{1 - \mathbf{E}^2 + B^2}{2(1 - E_2^2)}, \quad (2.38)$$

where electric field \mathbf{E} is given as

$$\mathbf{E} = E_1(x)\hat{i} + E_2(x)\hat{j}. \quad (2.39)$$

Three-dimensional analogue of Faraday's law is

$$\frac{\partial B}{\partial t} = -\epsilon_{0ij} \partial_i E, \quad (2.40)$$

which implies magnetic field B

$$B = B(x) \quad (2.41)$$

where $E_i = F_{i0}$, and $B = \epsilon_{0ij} F_{ij}/2$.

The potential (2.26) is

$$\begin{aligned} U_{\text{EM}}(T) &= -\frac{\mathcal{T}_2 E_1^2}{2\Pi_1^2(1 - E_2^2)} V(T)^2 \\ &= -\frac{\mathcal{T}_2 E_1^2}{2\Pi_1^2(1 - E_2^2)} \frac{1}{\cosh^2(T/T_0)}. \end{aligned} \quad (2.42)$$

When (2.28) $\lambda > 0$ ($E_2 < 1$), tachyon configurations are exactly same to that in kink with electric field case. However, when $\lambda < 0$ ($E_2 > 1$), the potential U_{EM} is flipped, the property of solutions changes. Thus, we will treat the case in which λ is negative.

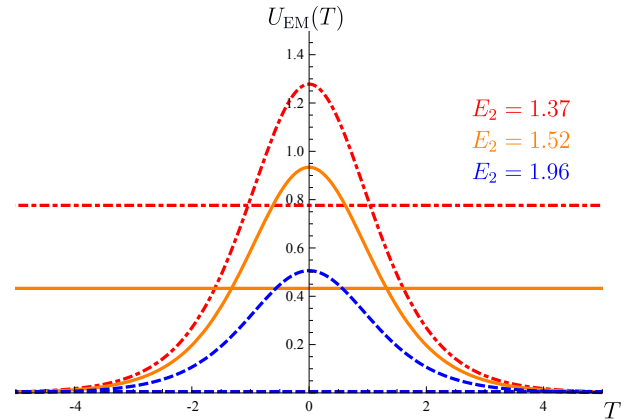


FIG. 9. Plot of potential $U(T)$ as the function of the tachyon field T (red dotted-dashed curve for electric field $E_2 = 1.37$, orange solid curve for electric field $E_2 = 1.52$, blue dashed curve for electric field $E_2 = 1.96$, respectively).

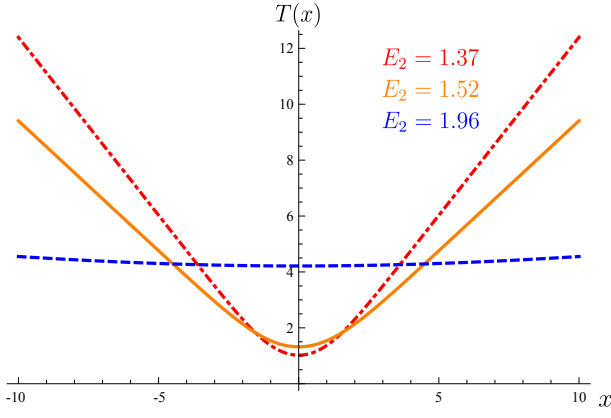


FIG. 10. Plot of the tachyon field $T(x)$ as the function of the position x (red dotted-dashed curve for electric field $E_2 = 1.37$, orange solid curve for electric field $E_2 = 1.52$, blue dashed curve for electric field $E_2 = 1.96$, respectively).

(i) When $0 < \mathcal{E}_{EM} < U_{EM}(0)$ ($0 < 1 - \mathbf{E}^2 + B^2 < (\mathcal{T}_2 E_1 / \Pi_1)^2$), there is a turning point at the origin ($x = 0$) as shown in Fig. 10. Then, the charge density is explicitly written as

$$\rho = \frac{\Pi_1(B^2 E_2^2 - E_1^2)}{E_1(E_2^2 - 1)} - \frac{\mathcal{T}_2^2 E_1}{\Pi_1(E_2^2 - 1)} \frac{1}{1 + (\chi^2 - 1) \cosh^2(x/\sigma)}, \quad (2.43)$$

with χ

$$\chi = \frac{\mathcal{T}_2^2 E_1^2}{\Pi_1^2 |1 - \mathbf{E}^2 + B^2|}, \quad (2.44)$$

and σ

$$\sigma = T_0 \sqrt{\left| \frac{1 - E_2^2}{1 - \mathbf{E}^2 + B^2} \right|}. \quad (2.45)$$

After taking $\mathcal{T}_2 = 1$, shapes of potential $U_{EM}(T)$ for various values of electric field E_2 are depicted in Fig. 9. The smaller electric field E_2 becomes, the more concave function in potential $U_{EM}(T)$. Then, profiles of tachyonic field $T(x)$ for various electric field E_2 and energy density are depicted in Fig. 10 and Fig. 11. Then, the configurational entropy $S_{C,EM}$ is depicted in Fig. 12. As electric field E_2 grows up, $S_{C,EM}$ starts at the minimum value ($S_{C,EM} = 3.8446$) and saturates to the maximum value ($S_{C,EM} = 3.8963$).

(ii) When $\mathcal{E}_{EM} = U_{EM}(0)$ ($1 - \mathbf{E}^2 + B^2 = (\mathcal{T}_2 E_1 / \Pi_1)^2$, as shown in Fig. 13.), there are the trivial ontop solution ($T(x) = 0$) and nontrivial tachyon half-kink solutions as shown in Fig. 14. Then, the charge density is given as

$$\rho = \frac{\Pi_1(B^2 E_2^2 - E_1^2)}{E_1(E_2^2 - 1)} - \frac{\mathcal{T}_2^2 E_1}{\Pi_1(E_2^2 - 1)} \frac{1}{1 + \exp(2x/\sigma)}. \quad (2.46)$$

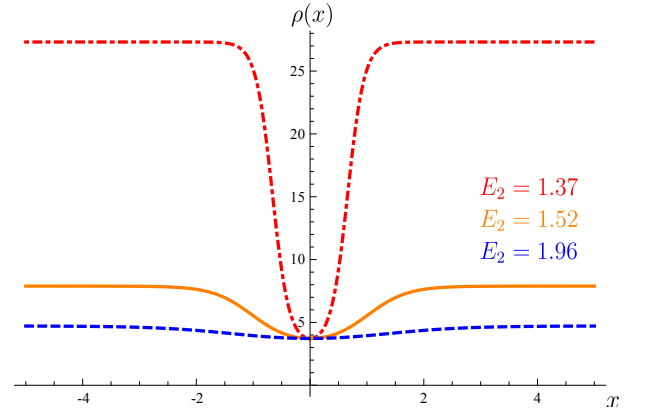


FIG. 11. Plot of energy density $\rho(x)$ as the function of the position x (red dotted-dashed curve for electric field $E_2 = 1.37$, orange solid curve for electric field $E_2 = 1.52$, blue dashed curve for electric field $E_2 = 1.96$, respectively).

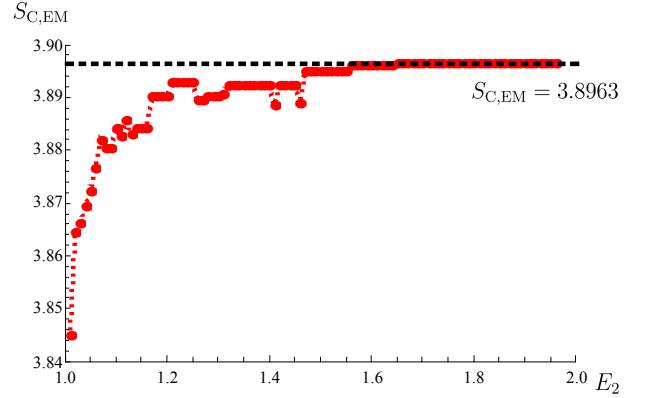


FIG. 12. Plot of tachyon configurational entropy with electromagnetic field $S_{C,EM}$ as the function of electric field E_2 .

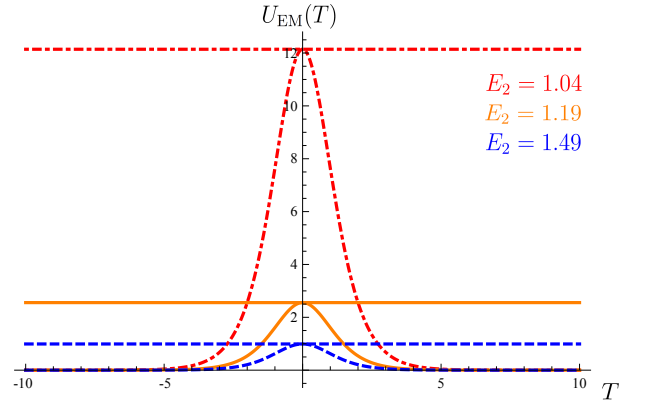


FIG. 13. Plot of potential $U(T)$ as the function of the tachyon field T (red dotted-dashed curve for electric field $E_2 = 1.04$, orange solid curve for electric field $E_2 = 1.19$, blue dashed curve for electric field $E_2 = 1.49$, respectively).

After taking $\mathcal{T}_2 = 1$, shapes of potential $U_{EM}(T)$ for various values of electric field E_2 are depicted in Fig. 13. The smaller electric field E_2 becomes, the more concave function in potential $U_{EM}(T)$. Then, profiles of tachyon

filed $T(x)$ for various electric field E_2 and energy density are depicted in Fig. 14 and Fig. 15. Then, the configurational entropy $S_{C,EM}$ is depicted in Fig. 16. As electric field E_2 grows up, $S_{C,EM}$ starts at the minimum value ($S_{C,EM} = 0.0002618$) and saturates to the maximum value ($S_{C,EM} = 3.7719$).

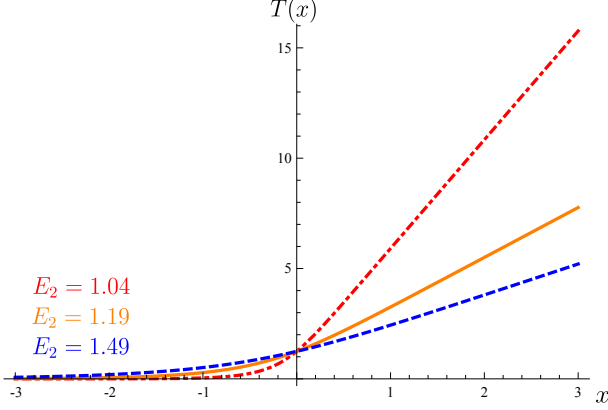


FIG. 14. Plot of the tachyon field $T(x)$ as the function of the position x (red dotted-dashed curve for electric field $E_2 = 1.04$, orange solid curve for electric field $E_2 = 1.19$, blue dashed curve for electric field $E_2 = 1.49$, respectively).

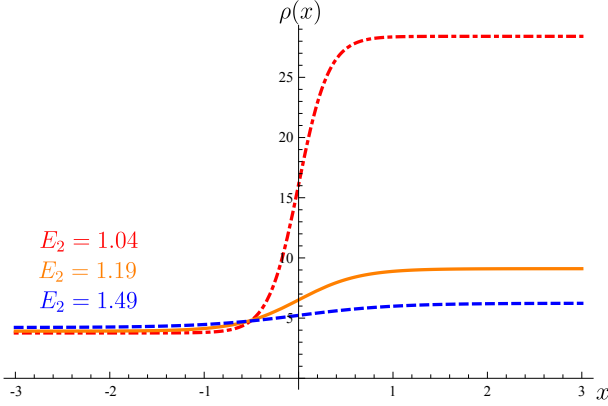


FIG. 15. Plot of energy density $\rho(x)$ as the function of the position x (red dotted-dashed curve for electric field $E_2 = 1.04$, orange solid curve for electric field $E_2 = 1.19$, blue dashed curve for electric field $E_2 = 1.49$, respectively).

(iii) When $\mathcal{E}_{EM} > U_{EM}(0)$ ($1 - \mathbf{E}^2 + B^2 > (\mathcal{T}_2 E_1 / \Pi_1)^2$, as shown in Fig 17.), there is hybrid of two half-kink solutions joined at the origin, as shown in Fig 18. Then, the charge density is given as

$$\rho = \frac{\Pi_1(B^2 E_2^2 - E_1^2)}{E_1(E_2^2 - 1)} \frac{1}{\mathcal{T}_2^2 E_1} \frac{1}{\Pi_1(E_2^2 - 1) 1 + (1 - \chi^2) \sinh^2(x/\sigma)}. \quad (2.47)$$

After taking $\mathcal{T}_2 = 1$, shapes of potential $U_{EM}(T)$ for various values of electric field E_2 are depicted in Fig. 13. The smaller electric field E_2 becomes, the more concave function in potential $U_{EM}(T)$. Then, profiles of tachyon

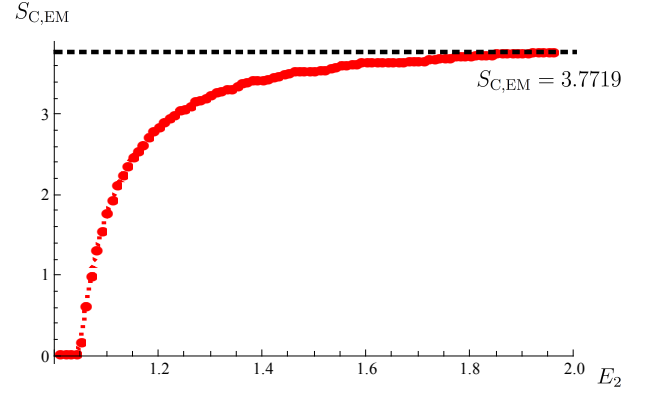


FIG. 16. Plot of tachyon configurational entropy with electromagnetic field $S_{C,EM}$ as the function of electric field E_2 .

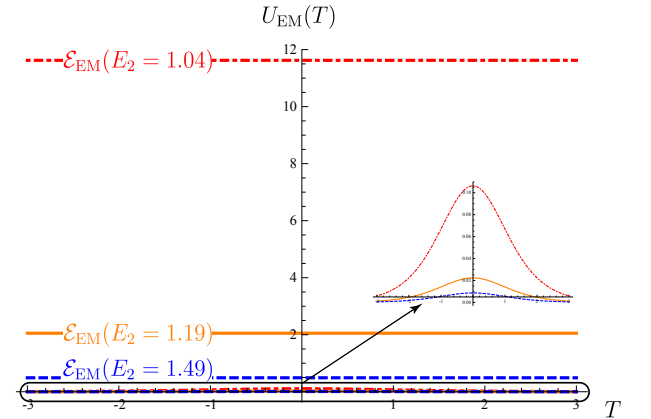


FIG. 17. Plot of potential $U(T)$ as the function of the tachyon field T (red dotted-dashed curve for electric field $E_2 = 1.04$, orange solid curve for electric field $E_2 = 1.19$, blue dashed curve for electric field $E_2 = 1.49$, respectively).

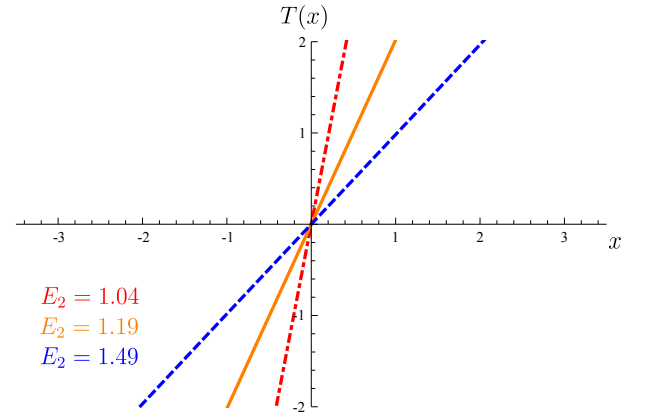


FIG. 18. Plot of the tachyon field $T(x)$ as the function of the position x (red dotted-dashed curve for electric field $E_2 = 1.04$, orange solid curve for electric field $E_2 = 1.19$, blue dashed curve for electric field $E_2 = 1.49$, respectively).

filed $T(x)$ for various electric field E_2 and energy density are depicted in Fig. 18. and Fig. 19. Then, the configurational entropy $S_{C,EM}$ is depicted in Fig. 20. As electric field E_2 grows up, $S_{C,EM}$ starts at the minimum

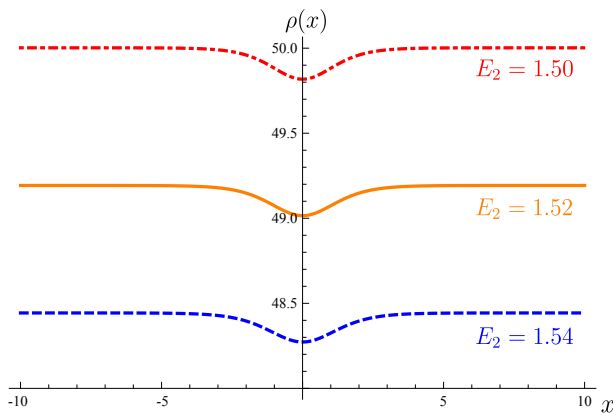


FIG. 19. Plot of energy density $\rho(x)$ as the function of the position x (red dotted-dashed curve for electric field $E_2 = 1.50$, orange solid curve for electric field $E_2 = 1.52$, blue dashed curve for electric field $E_2 = 1.54$, respectively).

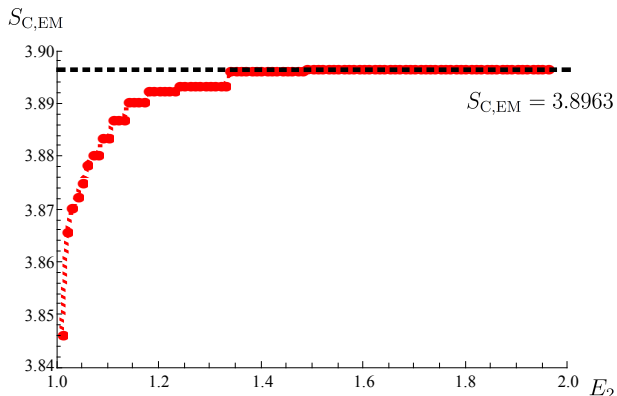


FIG. 20. Plot of tachyon configurational entropy with electromagnetic field $S_{C,EM}$ as the function of electric field E_2 .

value ($S_{C,EM} = 3.8459$) and saturates to the maximum value ($S_{C,EM} = 3.8963$).

III. CONCLUSION

We considered the tachyonic system coupled to Born-Infeld electromagnetism and investigated its configurational entropy. It was found that the configurational entropy saturates to the maximum value as the pressure of pure tachyonic field $-p_1$ grows up. We also showed that the configurational entropy in the presence of electromagnetic fields saturates to the maximum value as electric field E_2 increases. Interestingly, when the magnetic field is turned off, the magnitude of electric field E reaches the critical value. Then, the configurational entropy has the global minimum, which is related to the predominant tachyonic states.

ACKNOWLEDGEMENTS

This work was supported by Basic Science Research Program through the National Research Foundation of Korea (NRF) funded by the Ministry of Education, Science and Technology (NRF-2018R1D1A1B07049451).

-
- [1] A. Sen, JHEP **9808**, 012 (1998) [hep-th/9805170].
 - [2] A. Sen, JHEP **0204**, 048 (2002) [hep-th/0203211].
 - [3] A. Sen, JHEP **0207**, 065 (2002) [hep-th/0203265].
 - [4] A. Sen, Mod. Phys. Lett. A **17**, 1797 (2002) [hep-th/0204143].
 - [5] J. M. Cline, H. Firouzjahi and P. Martineau, JHEP **0211**, 041 (2002) [hep-th/0207156].
 - [6] G. N. Felder, L. Kofman and A. Starobinsky, JHEP **0209**, 026 (2002) [hep-th/0208019].
 - [7] G. N. Felder and L. Kofman, Phys. Rev. D **70**, 046004 (2004) [hep-th/0403073].
 - [8] N. Barnaby, JHEP **0407**, 025 (2004) [hep-th/0406120].
 - [9] N. D. Lambert, H. Liu and J. M. Maldacena, JHEP **0703**, 014 (2007) [hep-th/0303139].
 - [10] J. Kluson, JHEP **0401**, 019 (2004) [hep-th/0312086].
 - [11] C. j. Kim, Y. b. Kim and C. O. Lee, JHEP **0305**, 020 (2003) [hep-th/0304180].
 - [12] C. Kim, Y. Kim, O. K. Kwon and C. O. Lee, JHEP **0311**, 034 (2003) [hep-th/0305092].
 - [13] A. Sen, Phys. Rev. D **68**, 106003 (2003) [hep-th/0305011].
 - [14] M. Gleiser and N. Stamatopoulos, Phys. Lett. B **713**, 304 (2012) [arXiv:1111.5597 [hep-th]].
 - [15] M. Gleiser and N. Stamatopoulos, Phys. Rev. D **86**, 045004 (2012) [arXiv:1205.3061 [hep-th]].
 - [16] A. E. Bernardini and R. da Rocha, Phys. Lett. B **762**, 107 (2016) [arXiv:1605.00294 [hep-th]].
 - [17] A. E. Bernardini, N. R. F. Braga and R. da Rocha, Phys. Lett. B **765**, 81 (2017) [arXiv:1609.01258 [hep-th]].
 - [18] N. R. F. Braga and R. da Rocha, Phys. Lett. B **776**, 78 (2018) [arXiv:1710.07383 [hep-th]].
 - [19] N. Barbosa-Cendejas, R. Cartas-Fuentevilla, A. Herrera-Aguilar, R. R. Mora-Luna and R. da Rocha, Phys. Lett. B **782**, 607 (2018) [arXiv:1805.04485 [hep-th]].
 - [20] G. Karapetyan, Phys. Lett. B **786**, 418 (2018) [arXiv:1807.04540 [nucl-th]].
 - [21] N. R. F. Braga, L. F. Ferreira and R. Da Rocha, Phys. Lett. B **787**, 16 (2018) [arXiv:1808.10499 [hep-ph]].
 - [22] A. E. Bernardini and R. Da Rocha, Phys. Rev. D **98**, no. 12, 126011 (2018) [arXiv:1809.10055 [hep-th]].
 - [23] M. Gleiser and D. Sowinski, Phys. Lett. B **727**, 272 (2013) [arXiv:1307.0530 [hep-th]].

- [24] M. Gleiser and N. Graham, Phys. Rev. D **89**, no. 8, 083502 (2014) [arXiv:1401.6225 [astro-ph.CO]].
- [25] M. Gleiser and N. Jiang, Phys. Rev. D **92**, no. 4, 044046 (2015) [arXiv:1506.05722 [gr-qc]].
- [26] R. Casadio and R. da Rocha, Phys. Lett. B **763**, 434 (2016) [arXiv:1610.01572 [hep-th]].
- [27] N. R. F. Braga and R. da Rocha, Phys. Lett. B **767** (2017) 386 [arXiv:1612.03289 [hep-th]].
- [28] C. O. Lee, Phys. Lett. B **772**, 471 (2017) [arXiv:1705.09047 [gr-qc]].
- [29] M. Gleiser, M. Stephens and D. Sowinski, Phys. Rev. D **97**, no. 9, 096007 (2018) [arXiv:1803.08550 [hep-th]].
- [30] G. German, A. Herrera-Aguilar, D. Malagon-Morejon, R. R. Mora-Luna and R. da Rocha, JCAP **1302**, 035 (2013) [arXiv:1210.0721 [hep-th]].